



Published in final edited form as:

*J Mol Cell Cardiol.* 2016 May ; 94: 1–9. doi:10.1016/j.yjmcc.2016.03.006.

## Acyl CoA synthetase-1 links facilitated long chain fatty acid uptake to intracellular metabolic trafficking differently in hearts of male versus female mice

Joseph R. Goldenberg, BS<sup>a,b</sup>, Xuerong Wang, MD<sup>a</sup>, and E. Douglas Lewandowski, PhD<sup>a,b,c</sup>

<sup>a</sup>Center for Cardiovascular Research, University of Illinois College of Medicine at Chicago, 909 South Wolcott Avenue, Chicago, IL 60612, USA

<sup>b</sup>Department of Physiology and Biophysics, University of Illinois College of Medicine at Chicago, 835 South Wolcott Avenue, Chicago, IL 60612, USA

<sup>c</sup>Sanford Burnham Prebys Medical Discovery Institute, 6400 Sanger Road, Orlando, FL 32827, USA

### Abstract

**Rationale**—Acyl CoA synthetase-1 (ACSL1) is localized at intracellular membranes, notably the mitochondrial membrane. ACSL1 and female sex are suggested to indirectly facilitate lipid availability to the heart and other organs. However, such mechanisms in intact, functioning myocardium remain unexplored, and roles of ACSL1 and sex in the uptake and trafficking of fats are poorly understood.

**Objective**—To determine the potential for ACSL1 and sex-dependent differences in metabolic trapping and trafficking effects of long-chain fatty acids (LCFA) within cardiomyocytes of intact hearts.

**Methods and Results**—<sup>13</sup>C NMR of intact, beating mouse hearts, supplied <sup>13</sup>C palmitate, revealed 44% faster trans-sarcolemmal uptake of LCFA in male hearts overexpressing ACSL1 (MHC-ACSL1) than in non-transgenic (NTG) males (P<0.05). Acyl CoA content was elevated by ACSL1 overexpression, 404% in males and 164% in female, relative to NTG. Despite similar ACSL1 content, NTG females displayed faster LCFA uptake kinetics compared to NTG males, which was reversed by ovariectomy. NTG female LCFA uptake rates were similar to those in ACSL1 males and ACSL1 females. ACSL1 and female sex hormones both accelerated LCFA uptake without affecting triglyceride content or turnover. ACSL1 hearts contained elevated ceramide, particularly C22 ceramide in both sexes and specifically, C24 in males. ACSL1 also induced lower content of fatty acid transporter-6 (FATP6) indicating cooperative regulation with

---

Corresponding Author: E. Douglas Lewandowski, Ph.D., Sanford Burnham Prebys Medical Discovery Institute at Lake Nona, 6400 Sanger Road, Orlando, FL. 32827, Telephone: 407-745-2152, dougl@sbpdiscovery.org.

**Publisher's Disclaimer:** This is a PDF file of an unedited manuscript that has been accepted for publication. As a service to our customers we are providing this early version of the manuscript. The manuscript will undergo copyediting, typesetting, and review of the resulting proof before it is published in its final citable form. Please note that during the production process errors may be discovered which could affect the content, and all legal disclaimers that apply to the journal pertain.

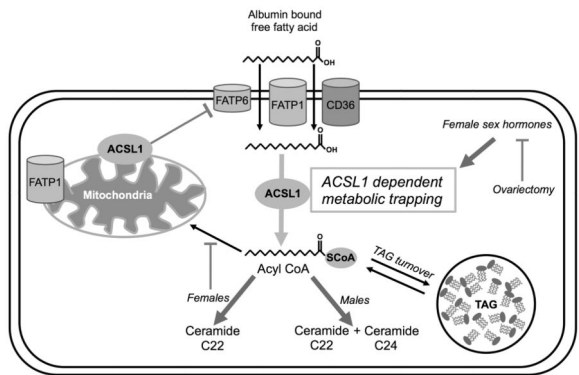
### DISCLOSURES

None.

ACSL1. Surprisingly, ACSL1 overexpression did not increase mitochondrial oxidation of exogenous palmitate, which actually dropped in female ACSL1 hearts.

**Conclusions**—ACSL1-mediated metabolic trapping of exogenous LCFA accelerates LCFA uptake rates, albeit to a lesser extent in females, which distinctly affects LCFA trafficking to acyl intermediates but not triglyceride storage or mitochondrial oxidation and is affected by female sex hormones.

**Graphical abstract**



**Keywords**

Heart; cardiac metabolism; fatty acid uptake; ceramide; triglyceride; acyl CoA synthetase

**1. INTRODUCTION**

Long-chain fatty acids (LCFA) serve numerous intracellular roles in the heart and homeostatic regulation of cellular lipids is crucial for physiologic heart function [1-3]. LCFA uptake is controlled by the kinetics of transport across the membrane, which is determined by the sarcolemmal fatty acid transporter CD36 [4-6]. Accelerated cardiac LCFA uptake from acute CD36 overexpression also contributed to increases in intramyocardial TAG turnover rates, albeit to a lesser extent. These findings underscore the importance of a protein affecting LCFA uptake and elucidating how uptake rates, and specifically, the action of ACSL1, influence trafficking of LCFA and the consequential production of acyl intermediates. Currently, whether ACSL1, a non-plasma membrane protein, indirectly facilitates LCFA uptake by metabolic trafficking of intracellular LCFA in the heart is not known.

Acyl CoA synthetase-1 (ACSL1), a protein reported to be localized at mitochondrial and endoplasmic reticular membranes, has been hypothesized to remotely affect LCFA uptake in mouse hearts, hepatocytes, adipocytes, epithelial cells, and *E. coli* through vectorial acylation as part of the mechanism “metabolic trapping” [7-15]. Despite the importance of ACSL1 in initiating intracellular lipid usage, the impact of ACSL1 on active fatty acid uptake rates and the consequences of altered uptake on cellular lipid utilization in the heart are not understood. Potentially, ACSL1 vectorial acylation can affect uptake rates by esterification of a LCFA to a coenzyme A thioester forming a fatty acyl CoA, which traps

the fatty acid in the cell, reduces intracellular free fatty acid (FFA) concentration, and increases the driving force for FFA transport across the plasma membrane [7,16].

Studies in hepatocytes, adipocytes, epithelial cells, and *E. coli*, all in culture, suggest ACSL1 to facilitate LCFA uptake. This effect of ACSL1 is suggested to occur via increased esterification and downstream storage of LCFA into lipid stores, such as triacylglyceride (TAG) [7-9,11-13,17,18]. In the mouse heart, cardiac-specific overexpression or deletion of ACSL1 has produced altered TAG and acyl CoA content, which is consistent with metabolic trapping effects by ACSL1 that may enhance LCFA uptake [14,15]. However, such studies from intact hearts have been limited to static measures of lipid content in frozen tissue. Conversely, the current study utilizes dynamic measures of the uptake and metabolic fate of labeled LCFA to directly explore ACSL1 effects in linking LCFA uptake rates and intracellular trafficking within intact, functioning hearts.

This study also examines the potential for ACSL1 to interact with sex differences in intracellular lipid handling, since female sex and estrogen affect both endogenous and exogenous lipids in the heart [19-21]. Human cardiac PET scans showed cardiac LCFA uptake is elevated in obese women and that female sex independently predicts fatty acid usage [22,23]. The effects of sex and the role of female hormones on ACSL1 or fatty acid metabolic trapping in the heart are currently unknown.

The current study is the first to examine the function of ACSL1 and the influence of female sex hormone on lipid uptake rates into cardiomyocytes and corresponding intracellular fates of exogenous LCFA within intact, functioning hearts. These studies were performed in a mouse model of cardiac-specific overexpression of acyl CoA synthetase-1 ( $\alpha$ MHC-ACSL1) [14]. We hypothesized that ACSL1 overexpression and female sex hormones synergistically accelerate cardiac fatty acid uptake kinetics and determine corresponding intracellular handling of acyl CoA. The findings suggest remote metabolic trapping effects of ACSL1 accelerates LCFA uptake and has local effects via intracellular LCFA trafficking, which is influenced by female sex hormones.

## 2. METHODS

### 2.1. Animals

Our study employed the low-overexpressing J3 line of  $\alpha$ MHC-ACSL1 mice, which were not lipid-overloaded and had no overt pathology. In contrast, high-overexpressing ACSL1 mouse lines had overwhelming cardiac lipotoxicity that reduced mouse life expectancy [14]. The non-lethal low-overexpressing mouse model allowed us to discern the subtleties of intracellular handling of acyl-derived lipids produced from modification of LCFA uptake kinetics. Age matched non-transgenic littermates were used as controls.

### 2.2. Ovariectomy

At 8-10 weeks of age female mice underwent surgery to remove ovaries or sham surgery. Surgeries were performed three weeks prior to any experiments, adequate time for changes in gene expression and protein levels [19].

### 2.3. Isolated heart perfusion

Hearts were excised for isolated, retrograde perfusion, as described [21,24,25]. A modified Krebs-Henseleit buffer containing 0.4 mmol/L  $^{12}\text{C}$  palmitate/albumin complex (3:1 molar ratio), 10 mmol/L glucose, and 1 mmol/L lactate was used to perfuse hearts. Cardiac function was monitored with a saline-filled, intraventricular balloon set at 5 mm diastolic pressure. Perfused hearts were situated in a 10 mm broadband probe in a vertical wide-bore (89mm) 14.1 T NMR magnet and maintained at 37 °C. Following experimental set up and stabilization of the preparations, the perfusate supply was then switched to similar buffer containing 0.4 mmol/L [ $^{13}\text{C}$ ] palmitate/albumin complex (3:1 molar ratio), 10 mmol/L glucose, and 1 mmol/L lactate during acquisition of dynamic-mode  $^{13}\text{C}$  NMR spectra over 30 minutes. Myocardial oxygen consumption was calculated from the oxygen concentration in the perfusate supplying the heart and the coronary effluent as previously described [26,27]. Hearts were rapidly frozen in liquid nitrogen cooled tongs following each protocol.

### 2.4. Nuclear Magnetic Resonance (NMR) spectroscopy and kinetic analysis of $^{13}\text{C}$ NMR data

Dynamic-mode  $^1\text{H}$  decoupled  $^{13}\text{C}$  NMR spectra were acquired signal averaged over two-minute intervals [21,24,25]. Background  $^{13}\text{C}$  natural abundance signal was then collected for digital subtraction from  $^{13}\text{C}$  enriched signals. The rate of  $^{13}\text{C}$  palmitate incorporation into TAG was calculated from the integrated signal intensity of the  $^{13}\text{C}$  resonance signal at 30.5 ppm, the TAG methylene carbons. Enrichment data is fitted using a bi-phasic kinetic model, encompassing a non-linear exponential fit for the rapid first phase of enrichment, followed by a linear fit for the slower second phase of enrichment after saturation of the early exponential phase, as described in Carley et al [4]. The initial, rapid exponential phase has been previously demonstrated to indirectly reflect transarcolemmal passage of  $^{13}\text{C}$  palmitate and initial esterification into TAG [4]. Non-linear regression analysis using one-phase association (GraphPad Prism) is used to fit the initial saturable exponential phase of  $^{13}\text{C}$  enrichment of TAG, to obtain  $\tau$ , the time constant. The second, slower phase of TAG enrichment is fitted by linear regression analysis (GraphPad Prism), and used to measure the relative rate of palmitate incorporation into TAG. Turnover of TAG is calculated from slope of the linear phase of TAG enrichment, in combination with endpoint TAG  $^{13}\text{C}$  enrichment and TAG content [4,21,24,28,29].

### 2.5. Myocardial lipid analysis

All lipids were extracted from frozen heart tissue and normalized to tissue protein concentration (BCA assay, Thermo Scientific). TAG was isolated using a modified Folch extraction as described [4,21,24,29]. Total TAG content was quantified with colorimetric kits (Wako Pure Chemical Industries). Ceramide species (C14, C16, C18, C18:1, C20, C22, C24, C24:1) were isolated using Sullards et al extraction [30] and quantified via LC-ESI-MS/MS as described previously [29]. Acyl CoA species (C14, C16, C18, C18:1, C18:2, C20, C20:4, C22, C24, C24:1) were isolated using Haynes et al extraction and quantified via LC-ESI-MS/MS protocol [31].

## 2.6. Western blot

Protein expression was measured by Western immunoblots on whole cell lysates as described [4,25,29]. Expression changes were quantified and normalized to intensity of loading control, calsequestrin.

## 2.7. Statistical analysis

All data are presented as mean  $\pm$  standard error of the mean (SEM). Two-way ANOVA or one-way ANOVA where appropriate followed by Tukey's post-hoc analysis was used to detect differences between groups (Graph Pad Prism). Differences were considered significant at a minimum of  $p < 0.05$ .

## 3. RESULTS

### 3.1. Cardiac function

Hemodynamics assessed from isolated perfused hearts was similar among experimental groups, indicating that cardiac function was not a determining variable of the metabolic observations report below. Mean values for rate-pressure-product, an index of mechanical work, ranged from 21,570 – 29,421 mm Hg  $\times$  BPM (SEM range: 3,023 – 5,003 mm Hg  $\times$  BPM) and were similar among all experimental groups. Additionally, the rates of pressure development and relaxation in the left ventricle, +dP/dt and -dP/dt, indexing contractility, were also similar among all groups (Supplemental Figure 1). Consistent with similar cardiac workloads across all experimental groups, myocardial oxygen consumption was also not significantly different: NTG male =  $30 \pm 6$ ; NTG female =  $30 \pm 12$ ; NTG OVX female =  $34 \pm 14$ ; ACSL1 male =  $29 \pm 4$ ; ACSL1 females =  $31 \pm 8$ ; ACSL1 OVX females =  $35 \pm 9$  ( $\mu\text{mole}/\text{min}/\text{g}$  dry wt., mean  $\pm$  SEM).

### 3.2. Kinetics of LCFA uptake and incorporation into TAG

Using dynamic proton-decoupled  $^{13}\text{C}$  NMR spectroscopy (Figure 1A) [4,29], we resolved, for the first time in the intact mouse heart, the biphasic nature of LCFA import into the steady state TAG pool with an initial rapid, saturable exponential component and a slower, linear component (Figures 1A and 1C). The initial exponential phase reflects LCFA uptake, with the apparent linear phase, representing TAG turnover as part of an extended exponential enrichment [4,21,24,28,29]. The  $R^2$  value was  $> 0.95$  for both the non-linear exponential and linear fit.

ACSL1 status and female sex affected the rate of the initial exponential phase ( $\tau$ , time constant) in perfused hearts (Figures 2A-D). ACSL1 males displayed a 44% lower  $\tau$  than NTG males ( $p < 0.01$ ) (Figures 2B and 2D). Female ACSL1 and NTG hearts had similar  $\tau$  values. Interestingly,  $\tau$  was 41% lower in female NTG than male NTG mice ( $p < 0.05$ ) demonstrating accelerated LCFA uptake rates in females at baseline (Figured 2C and 2D). Ovariectomy (OVX) increased  $\tau$  by 97% in NTG female mice ( $p < 0.01$ ), implicating a role for female sex hormones in faster LCFA uptake rates in female NTG hearts (Figured 2C and 2D). Female ACSL1 OVX hearts displayed values of  $\tau$  similar to that of female NTG OVX hearts. Overexpression of ACSL1 in ovariectomized female hearts was insufficient to overcome the increase in  $\tau$  resulting from removal of female sex hormones and did not

restore accelerated LCFA uptake in female hearts. ACSL1, albeit to a lesser extent in female ACSL1 hearts, and female sex hormones accelerated LCFA uptake rates in perfused hearts.

### 3.3. Intramyocardial Acyl CoA reflects ACSL1 overexpression

ACSL1 catalyzes CoA esterification to fatty acids forming acyl CoA. We quantified all acyl CoA species with a chain length of 14 to 24 as well as enrichment with labeled  $^{13}\text{C}$  in perfused hearts (Figures 3A-D). Total  $^{12}\text{C}$  and  $^{13}\text{C}$  acyl CoA content was 404% higher in male ACSL1 ( $p < 0.001$ ) and 164% higher in female ACSL1 ( $p < 0.05$ ) hearts compared to respective sex NTG hearts (Figure 3A). The content of  $^{13}\text{C}$  enriched acyl CoA was higher in male ACSL1 hearts compared to NTG hearts ( $p < 0.01$ , Figure 3B). Acyl CoA pool  $^{13}\text{C}$  percent enrichment did not change with ACSL1 expression (Figure 3C) despite a quantitative increase in  $^{13}\text{C}$  acyl CoA species (Figure 3B). This indicates lipolysis of the TAG pool was able to keep pace with the accelerated uptake and replenish  $^{12}\text{C}$  acyl chains to maintain equilibrium between  $^{12}\text{C}$  and  $^{13}\text{C}$  acyl CoA. ACSL1 overexpression lead to greater esterification of exogenously supplied U- $^{13}\text{C}$  palmitate to  $^{13}\text{C}$  acyl CoA and overall greater production of long-chain acyl CoAs.

### 3.4. Storage of LCFA into TAG is unaffected by LCFA uptake rates

The linear phase of  $^{13}\text{C}$  enrichment obtained from dynamic-mode  $^{13}\text{C}$  NMR spectra (Figure 1A), TAG content (Figure 4A), and final TAG  $^{13}\text{C}$  enrichment, quantified by LC-MS, was used to calculate turnover of the intramyocardial TAG pool (Figure 4B). Despite modifications in LCFA uptake kinetics by sex and ACSL1, LCFA esterification to TAG and turnover of the TAG pool remained unaffected across sexes and ACSL1 status. ACSL1 modified only the uptake dependent rate of TAG enrichment and not TAG turnover. These data demonstrate the independent actions of LCFA uptake to TAG synthesis and lipolysis [4].

### 3.5. Cardiac ACSL1 affects ceramide synthesis

Excess fatty acyl CoA that is not esterified into triglyceride may be converted into other acyl derivatives. Compared to respective NTG sex, ACSL1 overexpression lead to total ceramide that was 55% higher in male ACSL1 ( $p < 0.05$ ), 70% higher in female ACSL1 ( $p < 0.01$ ), and 47% in female ACSL1 OVX ( $p < 0.05$ ) hearts (Figure 4C). Specifically, ceramides C22 was elevated in all ACSL1 hearts versus the respective sex NTG group (Figure 4D). Very long-chain ceramide C24 was elevated only in male ACSL1 mice compared to same sex NTG groups. Additionally, ceramide C24 was significantly higher in male ACSL1 mice compared to female ACSL1 or female ACSL1 OVX groups. ACSL1 overexpression induced excess synthesis of total acyl derived long chain ceramides in the heart in all ACSL1 groups with sex influencing production of specific species.

### 3.6. ACSL1 does not channel fatty acids to cardiac mitochondrial beta-oxidation

ACSL1 has been identified at the outer mitochondrial membrane in addition to the endoplasmic reticulum [9,10,13,32,33]. Therefore, mitochondrial oxidation of LCFA was examined to determine if ACSL1 can channel LCFA to mitochondrial oxidation. In vitro  $^{13}\text{C}$  NMR of tissue extracts from perfused hearts showed  $\beta$ -oxidation of  $^{13}\text{C}$  palmitate to acetyl



CoA was not increased by ACSL1 overexpression, and was unexpectedly decreased in female ACSL1 hearts (Figure 4E). This latter finding in the female ACSL1 hearts indicates interactions between female sex hormone and ACSL1 in affecting LCFA contribution to beta-oxidation, but sex alone did not influence the fractional contribution of palmitate to acetyl CoA formation in NTG hearts. Overexpression of ACSL1 did not result in enhancement or channeling of LCFA into mitochondrial beta-oxidation.

The measure of relative contribution to the formation of acetyl-CoA, which in the current study indexes contributions from beta-oxidation of  $^{13}\text{C}$  enriched palmitate, is not the flux rate through beta-oxidation, but rather the relative contributions of each available fuel for entry into oxidative metabolism. As stated above, and as observed in previous studies, the actual oxidative rates in the mechanically-loaded, whole heart are driven by the energetic demand of mechanical work [24,25,29], and mechanical work was equivalent between groups (see 3.1 above and Supplemental Figure 1).

### 3.7. LCFA uptake kinetics and ACSL1 expression respond to female sex hormones

Protein content of ACSL1 was significantly higher as expected in ACSL1 transgenic hearts in all NTG vs ACSL1 comparisons ( $p < 0.0001$ , Figures 5A and 5B). Protein expression of ACSL1 in the transgenic hearts dwarfed the quantity of ACSL1 in NTG hearts and made between sex group comparisons for NTG hearts impossible. To determine if there exists baseline sex differences in ACSL1 expression that may explain the faster LCFA uptake kinetics observed in female NTG hearts, separate SDS-PAGE gels and western blots for NTG and ACSL1 overexpressing hearts were performed. In the separate western blot analysis, ACSL1 did not differ between male and female NTG hearts.

Interestingly, ACSL1 levels decreased in NTG females subject to ovariectomy (Figures 5C and 5D). The slower LCFA uptake rates in female NTG OVX hearts can be at least partially explained by interaction between female sex hormones and ACSL1. In overexpressing hearts, ACSL1 protein expression was higher in female hearts (Figures 5E and 5F). Though, the relative increase compared to male NTG hearts was similar for male ACSL1 hearts ( $p < 0.0001$ ) and for all within respective sex group comparisons (Figure 5B). Production of ovarian hormones is necessary for normal ACSL1 expression in females and correlates with LCFA uptake rates in female NTG hearts when ovarian hormones are removed.

### 3.8. Membrane fatty acid transporters response to ACSL1 expression

We examined a potential linkage between fatty acid metabolic trapping and expression of sarcolemmal fatty acid transporters. Epitope tagged ACSL1 and fatty acid transport protein-1 (FATP1) were co-immunoprecipitated from 3T3-L1 adipocytes and may work together to control fatty acid uptake [34]. We assayed protein content of FATP1, FATP6, and CD36 from frozen hearts (Figures 6A-F). Interestingly, ACSL1 overexpression decreased FATP6 significantly in transgenic hearts across sexes (Figures 6E and 6F;  $p < 0.05$  for male;  $p < 0.001$  for female and female OVX). FATP1 and CD36 levels were unaltered in all groups (Figures 6A-6D). This suggests ACSL1 negatively regulates FATP6 protein expression and may specifically work in coordination with FATP6 to regulate fatty acid uptake in the heart.

## 4. DISCUSSION

In this study we demonstrate for the first time the effects of ACSL1 dependent metabolic trapping of fatty acids and sex on LCFA uptake rates and utilization in the intact beating heart. Metabolic trapping is a mechanism by which non-transporter proteins affect LCFA uptake by vectorial acylation [7]. The FFA concentration gradient across the membrane increases through rapid conversion of intracellular FFA to fatty acyl CoA. Fatty acid metabolic trapping was previously only hypothesized in cells based on increased content of radiolabeled or fluorescent fatty acids in cells [7,9-11,13,16]. Here, with an *in vivo*, model we show accelerated trapping of fatty acids by ACSL1 resulted in greater LCFA uptake rates and FFA conversion to acyl CoA in ACSL1 overexpressing hearts (Figure 3A).

### 4.1. LCFA uptake and evidence of metabolic trapping in the heart

As previously identified, dynamic-mode  $^{13}\text{C}$  NMR of isolated hearts revealed two phases of TAG enrichment, each characterized by distinct kinetics (Figure 1C) [4]. Carley et al showed the initial  $^{13}\text{C}$  exponential phase of TAG enrichment is rapidly saturated and was modified by content of the sarcolemmal fatty acid translocase, CD36 [4]. This early, rapid exponential phase of enrichment reflects LCFA uptake across the sarcolemmal membrane. Consistent with that finding, *in vitro* studies support a rapid and saturable exponential phase of LCFA uptake in cardiomyocytes [5]. In the present study, ACSL1 overexpression accelerated the initial rapid, exponential enrichment phase, but the slower phase of apparent, linear  $^{13}\text{C}$  enrichment, associated with TAG turnover [4,21,24,28,29], remained similar among all experimental groups.

Interestingly, cardiac TAG content was unchanged in ACSL1 total body knockout mice [15], further supporting our result that ACSL1 does not shuttle active lipids to TAG synthesis. Though, TAG lipolysis may have been important in generating endogenous, intracellular  $^{12}\text{C}$  acyl chains to maintain equilibrium with  $^{13}\text{C}$  acyl CoA within the expanded acyl CoA pool that results from ACSL1 overexpression. The quantity of  $^{13}\text{C}$  acyl CoA species increased in male ACSL1 hearts, though the percent of  $^{13}\text{C}$  enriched acyl CoA was unaltered (Figures 3B and 3C). Thus, unlike the sarcolemmal transporter, CD36, the synthetase, ACSL1, links LCFA uptake to cellular utilization indirectly enhancing LCFA uptake by trapping of acyl units via esterification to CoA.

Ceramides have been implicated as mediators of cellular dysfunction in whole organ studies and in numerous cell types including cardiomyocytes, [29,35-39]. Ceramide overproduction may be derived from excess acyl CoA, the substrate for *de novo* ceramide synthesis [40], such as in diabetes when fatty acid uptake exceeds oxidation [41], or as in non-diabetic failing hearts when fatty acids are not stored in intracellular TAG stores and beta-oxidation is reduced [28,29,39,42]. The current results in the ACSL1 mouse demonstrate that an overabundance of intracellular acyl CoA is synthesized to acyl derived ceramides (Figures 4C and 4D). Male vs female sex influenced production of specific ceramide species in the ACSL1 mouse; notably C24 in male ACSL1 mice was higher than in female ACSL1 and female ACSL1 OVX mice. However, the current study does not suggest that these very long-chain ceramides were sufficiently abundant to induce cardiotoxicity to a level that would



produce any cardiac dysfunction or mortality in this low-overexpressing J3  $\alpha$ MHC-ACSL1 mouse strain, in contrast to the high-overexpressing O7 MHC-ACSL1 line [14].

Evidence exists in the literature for a link between specific very long-chain ceramides and membrane fatty acid transporter expression. Treatment of hepatocytes with exogenous C22 and C24 ceramides decreased CD36 expression [43]. Potentially, elevated C22 ceramides in the ACSL1 hearts are responsible for decreased FATP6 expression. The observed responses in ceramide and FATP6 content underscore the importance of studying the production of acyl-derived lipids in a non-pathogenic model of fatty acid metabolic trapping.

This study further supports the idea that cytosolic synthetases might interact with membrane transporters. Recombinant Myc-tagged ACSL1 was co-immunoprecipitated with FATP1 in 3T3-L1 adipocytes, alluding to a physical interaction [34]. Surprisingly, FATP6 protein decreased in all ACSL1 groups, but FATP1 and CD36 proteins were unchanged. In response to ACSL1 metabolic trapping driving LCFA across the membrane, possibly FATP6 expression decreased as compensation to reduce FFA membrane channels.

The decrease in FATP6 content may also be an adaptive response to overlapping synthetase function with ACSL1 CoA synthetase. FATP proteins have CoA synthetase capabilities in addition to their fatty acid transport functions [6,44,45]. Murine FATP isoforms expressed in yeast only formed acyl CoA from very long-chain fatty acids, C20:4 and C24, and not from a long-chain fatty acid C18:1, however C16 fatty acids were not examined [44]. Therefore, it is possible FATP synthetase substrate selectivity differs for individual LCFAs, such as C16 versus C18:1. Indeed, cells transfected with a human FATP6 expression vector displayed greater uptake of C16 than C8, C18:1, or C18:2 [45]. Redundancy between FATP6 preference for C16 fatty acids and overexpressed ACSL1 may have been the cause for FATP6 downregulation. Since CD36 and FATP1 were unchanged, ACSL1 appears to function cooperatively with CD36 and FATP1 to facilitate LCFA uptake. This observation is consistent with a previous *in vitro* study showing ACSL1 and CD36 synergy in oleate uptake [12]. Our study suggests a previously unknown cooperative regulation of LCFA uptake between membrane transport protein FATP6 and intracellular acyl chain activation mediated by changes in gene expression.

ACSL1 has been localized to the mitochondria outer membrane and based on ACSL1 knockout studies it might be expected that ACSL1 channels lipids into the mitochondria for beta-oxidation [10,13,15,16,33,46-48]. Studies of ACSL1 knockout mice, whole body or specific to heart muscle, skeletal muscle, liver, and adipose, revealed reduced LCFA oxidation [15,46-48]. In contrast, *in vitro* overexpression of ACSL1 [9] and our data presented here with an *in vivo* ACSL1 overexpression model did not result in enhanced LCFA oxidation. Our finding indicates that the reduced LCFA oxidation in ACSL1 deficient tissues is more likely to be the consequence of reduced LCFA uptake and activation to the CoA ester than due to channeling of LCFA into oxidative metabolism.

#### 4.2. Sex differences and female hormone-dependent LCFA trafficking

Differences in fatty acid uptake were observed under baseline conditions between male and female NTG hearts. Normal female NTG hearts had faster LCFA uptake kinetics in

comparison to normal males (Figure 2A and 2D). Although both acyl CoA and ACSL1 protein contents were similar between NTG males and NTG females (Figures 4A, 6C, and 6D), ovariectomy resulted in slower LCFA uptake rates and lower ACSL1 protein (Figures 2C, 2D, 5C and 5D). Loss of female hormones reduced ACSL1 facilitated metabolic trapping in females, though overexpression of ACSL1 did not restore accelerated LCFA uptake in OVX mice. Additional factors are likely involved in mediating accelerated LCFA uptake rates in females, since ACSL1 expression in female NTG hearts was not higher and ACSL1 overexpression was unable to overcome the loss of female sex hormones. Though, physiologic accelerated LCFA uptake rates in females are at least partially mediated by ACSL1 expression, which is dependent on normal female sex hormone production. This is consistent with published data indicating that hearts of females have a much more active lipid metabolism than that of males [21-23]. Surprisingly, ACSL1 expression was higher in female transgenic hearts than male transgenic hearts, though ACSL1 expression was similarly increased in all transgenic groups ( $P < 0.0001$ , Figures 6A, 6B, 6E, and 6F). Potentially, this could be due to unexamined sex hormone interaction with the  $\alpha$ MHC promoter activity. Androgens may be involved since female ACSL OVX hearts had similarly higher expression levels as female ACSL1 hearts. The current findings underscore the need for future studies to examine the impact of cellular lipid utilization on established sex differences in cardiac disease.

ACSL1-mediated trafficking of LCFA differed between males and females. Unexpectedly, ACSL1 overexpression induced a drop in exogenous palmitate oxidation in female ACSL1 hearts (Figure 4E). The remaining acetyl CoA production likely comes from  $^{12}\text{C}$  fatty acids supplied by endogenous TAG lipolysis as well as glucose and lactate in the perfusate. The decreased contribution of palmitate to acetyl CoA production in female ACSL1 hearts is therefore like the result of interactions between female sex hormones and ACSL1 activity. The data suggest that ACSL1 trafficks exogenous  $^{13}\text{C}$  palmitate toward an alternate metabolic fate other than oxidation. Indeed, ACSL1 increased ceramide production in males and females, but with sex differences in specific ceramides, suggesting both ACSL1 and female sex hormones affect the specific pool of excess acyl CoA derived from ACSL1 that is upstream of transport into mitochondria and available for ceramide synthesis. Thus, female sex hormones and ACSL1 are interactive.

The impact of lipid metabolism based sex differences on cardiac pathology or conditions of metabolic stress have only recently been studied [21,23,49]. Peterson et al, demonstrated female sex was an independent predictor of palmitate uptake and utilization in healthy and obese subjects [22]. Female sex predicted greater cardiac inefficiency and only in obese women increasing BMI positively correlated to  $\text{MVO}_2$  [22,50]. In a separate study, female non-obese type 2 diabetic subjects had greater left ventricle fatty acid oxidation, esterification, and overall utilization despite taking more lipid lowering therapies than male non-obese type 2 diabetic patients [23]. Further, in female mice cardiac TAG turnover is more dynamic and resilient to the chronic metabolic stress of calorie restriction [21]. An important mechanism contributing to greater female LCFA uptake may be increased expression of LPL, which was found to be transcriptionally activated by the estrogen receptor [19]. As a result of greater intracellular lipid availability from exogenous and endogenous lipid sources females have a greater dependence on LCFA in the heart. The data

that we presented here fits with previous human and animal studies demonstrating female sex may augment lipid utilization through accelerated LCFA uptake.

In other organs, a complex network of crosstalk between PPAR $\alpha$  and estrogen exists [51-56]. Thus, interactions between female sex hormone and PPAR $\alpha$  target gene expression, that include *Acs11*, may contribute to the currently observed sex differences [57,58]. Hepatic lipid accumulation and death resulted in male PPAR $\alpha$   $-/-$  mice treated with the CPT1 inhibitor, etomoxir, but not in female PPAR $\alpha$   $-/-$  mice treated with etomoxir [56]. Potentially, interactions between PPAR $\alpha$  and estrogen at the transcriptional and perhaps the post-transcriptional level may underlie our results documenting interactions between female sex hormones and ACSL1 [56]. It is possible ovariectomy induced changes in circulating lipids that may have affected activity of PPAR $\alpha$  and thus transcription of lipid transporters in the heart that were not measured. Notwithstanding this, our measurements of fatty acid uptake rates in *ex vivo* beating hearts demonstrated intrinsic changes occurred in female and female OVX hearts. Future studies are needed to clarify interactions between estrogen, PPAR $\alpha$ , and PPAR $\alpha$  gene products.

In conclusion, we quantified the remote affects of ACSL1 on LCFA uptake rates (Figure 2A-2D) and intracellular lipid trafficking (Figures 3A-3D and 4A-4E) as well as basal sex differences in LCFA uptake into the heart that are at least partially explained by ovarian hormone regulation of the metabolic trapping effects of ACSL1 (Figures 5C and 5D). Ovariectomy lowered ACSL1 expression thus slowing LCFA uptake kinetics and indicating the faster kinetics of LCFA uptake in females are affected by ovarian hormone regulation of ACSL1 metabolic trapping. However, the data suggest that female sex hormones affect LCFA uptake through additional processes other than ACSL1 metabolic trapping alone. The effect of ACSL1 overexpression on female uptake rates was not as evident, since uptake kinetics were similar between female NTG and female ACSL1 hearts (Figure 2D). Changes in cardiac LCFA uptake in female mice resulting from manipulation of ovarian hormones did not affect intracellular acyl CoA content (Figures 3A). Therefore, the exponential rate of stable isotope enrichment is not a direct index of ACSL1 activity, but is responsive to the degree of ACSL1 expression and resultant metabolic trapping effects of this CoA synthase. ACSL1 expression level induced a decrease in sarcolemmal FATP6 transporter expression revealing a role for cooperative regulation between sarcolemmal protein expression and intracellular synthetases (Figure 6A-6F). Overall, ACSL1 and female sex hormones play a critical role in fatty acid metabolism and cellular responses to the modifications of these physiologic factors.

## Supplementary Material

Refer to Web version on PubMed Central for supplementary material.

## Acknowledgments

### SOURCES OF FUNDING

This work was supported by National Institute of Health grants R01-HL113057 and R01-HL49244 and an American Heart Association Predoctoral Fellowship 15PRE21180004.

## GLOSSARY

<b>ACSL1</b>	Acyl CoA synthetase-1
<b>CoA</b>	Coenzyme A
<b>FATP</b>	Fatty acid transport protein
<b>LCFA</b>	Long-chain fatty acid
<b>OVX</b>	Ovariectomy
<b>NTG</b>	Non-transgenic
<b>TAG</b>	Triacylglyceride

## REFERENCES

- Doenst T, Nguyen TD, Abel ED. Cardiac metabolism in heart failure: implications beyond ATP production. *Circ. Res.* 2013; 113:709–24. [PubMed: 23989714]
- Kolwicz SC, Purohit S, Tian R. Cardiac metabolism and its interactions with contraction, growth, and survival of cardiomyocytes. *Circ. Res.* 2013; 113:603–16. [PubMed: 23948585]
- Carley AN, Taegtmeier H, Lewandowski ED. Matrix revisited: mechanisms linking energy substrate metabolism to the function of the heart. *Circ. Res.* 2014; 114:717–29. [PubMed: 24526677]
- Carley AN, Bi J, Wang X, Banke NH, Dyck JRB, O'Donnell JM, et al. Multiphasic triacylglycerol dynamics in the intact heart during acute in vivo overexpression of CD36. *J. Lipid Res.* 2013; 54:97–106. [PubMed: 23099442]
- Carley AN, Kleinfeld AM. Fatty acid (FFA) transport in cardiomyocytes revealed by imaging unbound FFA is mediated by an FFA pump modulated by the CD36 protein. *J. Biol. Chem.* 2011; 286:4589–97. [PubMed: 21147770]
- Glatz JFC, Luiken JJFP, Bonen A. Membrane fatty acid transporters as regulators of lipid metabolism: Implications for metabolic disease. *Physiol. Rev.* 2010; 90:367–417. [PubMed: 20086080]
- Füllekrug J, Ehehalt R, Poppelreuther M. Outlook: membrane junctions enable the metabolic trapping of fatty acids by intracellular acyl-CoA synthetases. *Front. Physiol.* 2012; 3:401. [PubMed: 23087649]
- Zhan, T.; Poppelreuther, M.; Ehehalt, R.; Füllekrug, J. Overexpressed FATP1, ACSVL4/FATP4 and ACSL1 increase the cellular fatty acid uptake of 3T3-L1 adipocytes but are localized on intracellular membranes. In: Soldati, T., editor. *PLoS One*. Vol. 7. Public Library of Science; 2012. p. e45087
- Li LO, Mashek DG, An J, Doughman SD, Newgard CB, Coleman RA. Overexpression of rat long chain acyl-coa synthetase 1 alters fatty acid metabolism in rat primary hepatocytes. *J. Biol. Chem.* 2006; 281:37246–55. [PubMed: 17028193]
- Milger K, Herrmann T, Becker C, Gotthardt D, Zickwolf J, Ehehalt R, et al. Cellular uptake of fatty acids driven by the ER-localized acyl-CoA synthetase FATP4. *J. Cell Sci.* 2006; 119:4678–88. [PubMed: 17062637]
- Overath P, Pauli G, Schairer HU. Fatty acid degradation in *Escherichia coli*. An inducible acyl-CoA synthetase, the mapping of old-mutations, and the isolation of regulatory mutants. *Eur. J. Biochem.* 1969; 7:559–74. [PubMed: 4887396]
- Schneider, H.; Staudacher, S.; Poppelreuther, M.; Stremmel, W.; Ehehalt, R.; Füllekrug, J. *Arch. Biochem. Biophys.* Elsevier Inc.; 2014. Protein mediated fatty acid uptake: Synergy between CD36/FAT-facilitated transport and acyl-CoA synthetase-driven metabolism.
- Krammer J, Digel M, Ehehalt F, Stremmel W, Füllekrug J, Ehehalt R. Overexpression of CD36 and acyl-CoA synthetases FATP2, FATP4 and ACSL1 increases fatty acid uptake in human hepatoma cells. *Int. J. Med. Sci.* 2011; 8:599–614. [PubMed: 22022213]

14. Chiu, H-C.; Kovacs, A.; Ford, D a; Hsu, F-F.; Garcia, R.; Herrero, P., et al. *J. Clin. Invest.* Vol. 107. American Society for Clinical Investigation; 2001. A novel mouse model of lipotoxic cardiomyopathy; p. 813-22.
15. Ellis JM, Mentock SM, Depetrillo MA, Koves TR, Sen S, Watkins SM, et al. Mouse cardiac acyl coenzyme a synthetase 1 deficiency impairs Fatty Acid oxidation and induces cardiac hypertrophy. *Mol. Cell. Biol.* 2011; 31:1252–62. [PubMed: 21245374]
16. Cooper DE, Young PA, Klett EL, Coleman RA. Physiological Consequences of Compartmentalized Acyl-CoA Metabolism. *J. Biol. Chem.* 2015; 290:20023–31. [PubMed: 26124277]
17. Mashek DG, Li LO, Coleman RA. Long-chain acyl-CoA synthetases and fatty acid channeling. *Future Lipidol.* 2007; 2:465–76. [PubMed: 20354580]
18. Gargiulo CE, Stuhlsatz-Krouper SM, Schaffer JE. Localization of adipocyte long-chain fatty acyl-CoA synthetase at the plasma membrane. *J. Lipid Res.* 1999; 40:881–92. [PubMed: 10224157]
19. Liu, D.; Deschamps, A.; Korach, K.S.; Murphy, E. *Endocrinology.* Vol. 149. The Endocrine Society; 2008. Estrogen-enhanced gene expression of lipoprotein lipase in heart is antagonized by progesterone; p. 711-6.
20. Murphy E. Estrogen signaling and cardiovascular disease. *Circ. Res.* 2011; 109:687–96. [PubMed: 21885836]
21. Banke, NH.; Yan, L.; Pound, KM.; Dhar, S.; Reinhardt, H.; De Lorenzo, MS., et al. *J. Mol. Cell. Cardiol.* Vol. 52. Elsevier B.V.; 2012. Sexual dimorphism in cardiac triacylglyceride dynamics in mice on long term caloric restriction; p. 733-40.
22. Peterson LR, Soto PF, Herrero P, Mohammed BS, Avidan MS, Schechtman KB, et al. Impact of gender on the myocardial metabolic response to obesity. *JACC. Cardiovasc. Imaging.* 2008; 1:424–33. [PubMed: 19356462]
23. Peterson LR, Saeed IM, McGill JB, Herrero P, Schechtman KB, Gunawardena R, et al. Sex and type 2 diabetes: obesity-independent effects on left ventricular substrate metabolism and relaxation in humans. *Obesity (Silver Spring).* 2012; 20:802–10. [PubMed: 21818149]
24. Banke NH, Wende AR, Leone TC, O'Donnell JM, Abel ED, Kelly DP, et al. Preferential oxidation of triacylglyceride-derived fatty acids in heart is augmented by the nuclear receptor PPARalpha. *Circ. Res.* 2010; 107:233–41. [PubMed: 20522803]
25. Banke NH, Lewandowski ED. Impaired cytosolic NADH shuttling and elevated UCP3 contribute to inefficient citric acid cycle flux support of postischemic cardiac work in diabetic hearts. *J. Mol. Cell. Cardiol.* 2015; 79:13–20. [PubMed: 25450611]
26. Lewandowski ED. Nuclear magnetic resonance evaluation of metabolic and respiratory support of work load in intact rabbit hearts. *Circ. Res.* 1992; 70:576–82. [PubMed: 1537093]
27. Lewandowski ED, Chari MV, Roberts R, Johnston DL. NMR studies of beta-oxidation and short-chain fatty acid metabolism during recovery of reperfused hearts. *Am. J. Physiol.* 1991; 261:H354–63. [PubMed: 1877663]
28. O'Donnell JM, Fields AD, Sorokina N, Lewandowski ED. The absence of endogenous lipid oxidation in early stage heart failure exposes limits in lipid storage and turnover. *J. Mol. Cell. Cardiol.* 2008; 44:315–22. [PubMed: 18155232]
29. Lahey R, Wang X, Carley AN, Lewandowski ED. Dietary Fat Supply to Failing Hearts Determines Dynamic Lipid Signaling for Nuclear Receptor Activation and Oxidation of Stored Triglyceride. *Circulation.* 2014; 130:1790–9. [PubMed: 25266948]
30. Sullards MC, Liu Y, Chen Y, Merrill AH. Analysis of mammalian sphingolipids by liquid chromatography tandem mass spectrometry (LC-MS/MS) and tissue imaging mass spectrometry (TIMS). *Biochim. Biophys. Acta.* 2011; 1811:838–53. [PubMed: 21749933]
31. Haynes CA, Allegood JC, Sims K, Wang EW, Sullards MC, Merrill AH. Quantitation of fatty acyl-coenzyme As in mammalian cells by liquid chromatography-electrospray ionization tandem mass spectrometry. *J. Lipid Res.* 2008; 49:1113–25. [PubMed: 18287618]
32. Lewin TM, Kim JH, Granger D a, Vance JE, Coleman R a. Acyl-CoA synthetase isoforms 1, 4, and 5 are present in different subcellular membranes in rat liver and can be inhibited independently. *J. Biol. Chem.* 2001; 276:24674–9. [PubMed: 11319232]

33. Distler AM, Kerner J, Peterman SM, Hoppel CL. A targeted proteomic approach for the analysis of rat liver mitochondrial outer membrane proteins with extensive sequence coverage. *Anal. Biochem.* 2006; 356:18–29. [PubMed: 16876102]
34. Richards MR, Harp JD, Ory DS, Schaffer JE. Fatty acid transport protein 1 and long-chain acyl coenzyme A synthetase 1 interact in adipocytes. *J. Lipid Res.* 2006; 47:665–72. [PubMed: 16357361]
35. Bielawska AE, Shapiro JP, Jiang L, Melkonyan HS, Piot C, Wolfe CL, et al. Ceramide is involved in triggering of cardiomyocyte apoptosis induced by ischemia and reperfusion. *Am. J. Pathol.* 1997; 151:1257–63. [PubMed: 9358751]
36. Aflaki E, Doddapattar P, Radovi B, Povoden S, Kolb D, Vuji N, et al. C16 ceramide is crucial for triacylglycerol-induced apoptosis in macrophages. *Cell Death Dis.* 2012; 3:e280. [PubMed: 22419109]
37. Bikman BT, Summers SA. Ceramides as modulators of cellular and whole-body metabolism. *J. Clin. Invest.* 2011; 121:4222–30. [PubMed: 22045572]
38. Park T-S, Hu Y, Noh H-L, Drosatos K, Okajima K, Buchanan J, et al. Ceramide is a cardiotoxin in lipotoxic cardiomyopathy. *J. Lipid Res.* 2008; 49:2101–12. [PubMed: 18515784]
39. Chokshi A, Drosatos K, Cheema FH, Ji R, Khawaja T, Yu S, et al. Ventricular assist device implantation corrects myocardial lipotoxicity, reverses insulin resistance, and normalizes cardiac metabolism in patients with advanced heart failure. *Circulation.* 2012; 125:2844–53. [PubMed: 22586279]
40. Holland WL, Summers SA. Sphingolipids, insulin resistance, and metabolic disease: new insights from in vivo manipulation of sphingolipid metabolism. *Endocr. Rev.* 2008; 29:381–402. [PubMed: 18451260]
41. Boudina S, Abel ED. Diabetic Cardiomyopathy Revisited. *Circulation.* 2007; 115:3213–23. [PubMed: 17592090]
42. Sorokina N, O'Donnell JM, McKinney RD, Pound KM, Woldegiorgis G, LaNoue KF, et al. Recruitment of compensatory pathways to sustain oxidative flux with reduced carnitine palmitoyltransferase I activity characterizes inefficiency in energy metabolism in hypertrophied hearts. *Circulation.* 2007; 115:2033–41. [PubMed: 17404155]
43. Park W-J, Park J-W, Merrill AH, Storch J, Pewzner-Jung Y, Futerman AH. Hepatic fatty acid uptake is regulated by the sphingolipid acyl chain length. *Biochim. Biophys. Acta.* 2014; 1841:1754–66. [PubMed: 25241943]
44. DiRusso CC, Li H, Darwis D, Watkins PA, Berger J, Black PN. Comparative biochemical studies of the murine fatty acid transport proteins (FATP) expressed in yeast. *J. Biol. Chem.* 2005; 280:16829–37. [PubMed: 15699031]
45. Gimeno RE, Ortegon AM, Patel S, Punreddy S, Ge P, Sun Y, et al. Characterization of a heart-specific fatty acid transport protein. *J. Biol. Chem.* 2003; 278:16039–44. [PubMed: 12556534]
46. Li LO, Grevengoed TJ, Paul DS, Ilkayeva O, Koves TR, Pascual F, et al. Compartmentalized Acyl-CoA Metabolism in Skeletal Muscle Regulates Systemic Glucose Homeostasis. *Diabetes.* 2015; 64:23–35. [PubMed: 25071025]
47. Ellis JM, Li LO, Wu P-C, Koves TR, Ilkayeva O, Stevens RD, et al. Adipose acyl-CoA synthetase-1 directs fatty acids toward beta-oxidation and is required for cold thermogenesis. *Cell Metab.* 2010; 12:53–64. [PubMed: 20620995]
48. Li LO, Ellis JM, Paich HA, Wang S, Gong N, Altschuller G, et al. Liver-specific loss of long chain acyl-CoA synthetase-1 decreases triacylglycerol synthesis and beta-oxidation and alters phospholipid fatty acid composition. *J. Biol. Chem.* 2009; 284:27816–26. [PubMed: 19648649]
49. Wittnich C, Tan L, Wallen J, Belanger M. Sex differences in myocardial metabolism and cardiac function: an emerging concept. *Pflugers Arch.* 2013; 465:719–29. [PubMed: 23404619]
50. Peterson LR, Herrero P, Schechtman KB, Racette SB, Waggoner AD, Kisrieva-Ware Z, et al. Effect of obesity and insulin resistance on myocardial substrate metabolism and efficiency in young women. *Circulation.* 2004; 109:2191–6. [PubMed: 15123530]
51. Jeong S, Han M, Lee H, Kim M, Kim J, Nicol CJ, et al. Effects of fenofibrate on high-fat diet-induced body weight gain and adiposity in female C57BL/6J mice. *Metabolism.* 2004; 53:1284–9. [PubMed: 15375783]



52. Yoon M, Jeong S, Nicol CJ, Lee H, Han M, Kim J-J, et al. Fenofibrate regulates obesity and lipid metabolism with sexual dimorphism. *Exp. Mol. Med.* 2002; 34:481–8. [PubMed: 12526091]
53. Jeong S, Yoon M. Inhibition of the actions of peroxisome proliferator-activated receptor alpha on obesity by estrogen. *Obesity (Silver Spring)*. 2007; 15:1430–40. [PubMed: 17557980]
54. Lee, H.; Yoon, M. *Animal Cells Syst.* (Seoul). Vol. 17. Taylor & Francis; 2013. 17 $\beta$ -estradiol inhibits PPAR $\alpha$  of skeletal muscle; p. 331-40.
55. Keller H, Givel F, Perroud M, Wahli W. Signaling cross-talk between peroxisome proliferator-activated receptor/retinoid X receptor and estrogen receptor through estrogen response elements. *Mol. Endocrinol.* 1995; 9:794–804. [PubMed: 7476963]
56. Djouadi F, Weinheimer CJ, Saffitz JE, Pitchford C, Bastin J, Gonzalez FJ, et al. A gender-related defect in lipid metabolism and glucose homeostasis in peroxisome proliferator-activated receptor alpha-deficient mice. *J. Clin. Invest.* 1998; 102:1083–91. [PubMed: 9739042]
57. Schoonjans K, Staels B, Grimaldi P, Auwerx J. Acyl-CoA synthetase mRNA expression is controlled by fibric-acid derivatives, feeding and liver proliferation. *Eur. J. Biochem.* 1993; 216:615–22. [PubMed: 8375397]
58. Martin G, Schoonjans K, Lefebvre A-M, Staels B, Auwerx J. Coordinate Regulation of the Expression of the Fatty Acid Transport Protein and Acyl-CoA Synthetase Genes by PPAR and PPAR Activators. *J. Biol. Chem.* 1997; 272:28210–7. [PubMed: 9353271]

**HIGHLIGHTS**

- ACSL1 and female sex hormones accelerate fatty acid uptake rates in beating hearts
- Faster female LCFA uptake rates require sex hormone-dependent ACSL1 expression
- ACSL1 increases acyl derivative conversion to ceramide; no changes to TAG storage
- Lipid trafficking of acyl derivatives differs between males and females

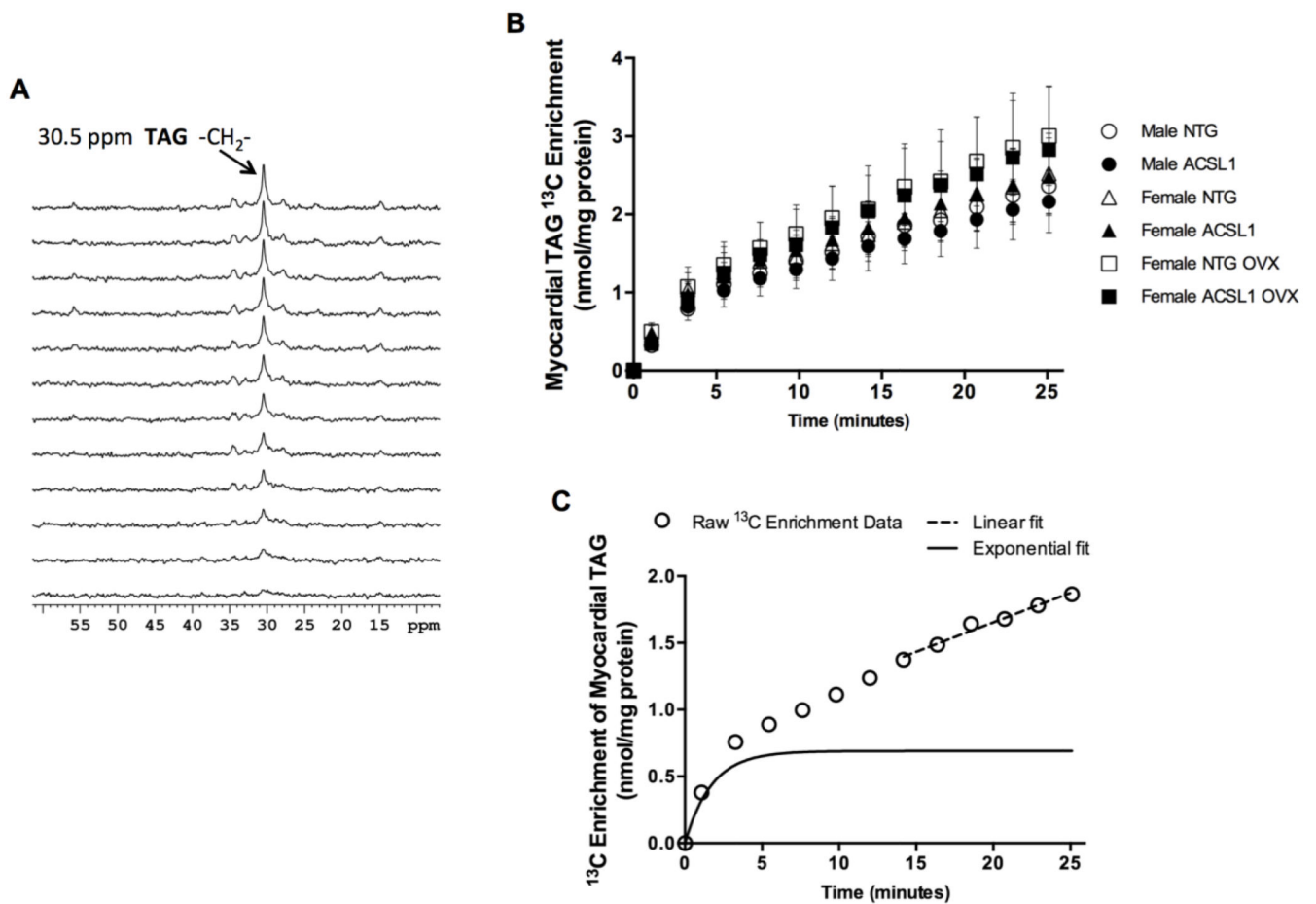


**Figure 1. Two distinct kinetic phases of <sup>13</sup>C palmitate incorporation into myocardial triacylglyceride**

(A) Dynamic-mode <sup>13</sup>C NMR proton-decoupled spectra (2 min each) acquired from an isolated, intact beating heart displaying progressive incorporation of [U-<sup>13</sup>C] palmitate in triacylglyceride (TAG). Resonance peak at 30.5 ppm corresponds to the methylene carbon of TAG. (B). Enrichment of TAG with <sup>13</sup>C over time for each experiment group: Male NTG n = 10, male ACSL1 n = 10, female NTG n = 8, female ACSL1 n = 8, female NTG OVX n = 5, female ACSL1 OVX n = 10. (C) Representative enrichment curve from individual perfused female ACSL1 mouse heart displaying multi-kinetic features. Subtraction of the linear component (dotted line) from the raw enrichment data demonstrates the initial exponential phase, as previously described (solid black line). See Supplemental Figure 2.

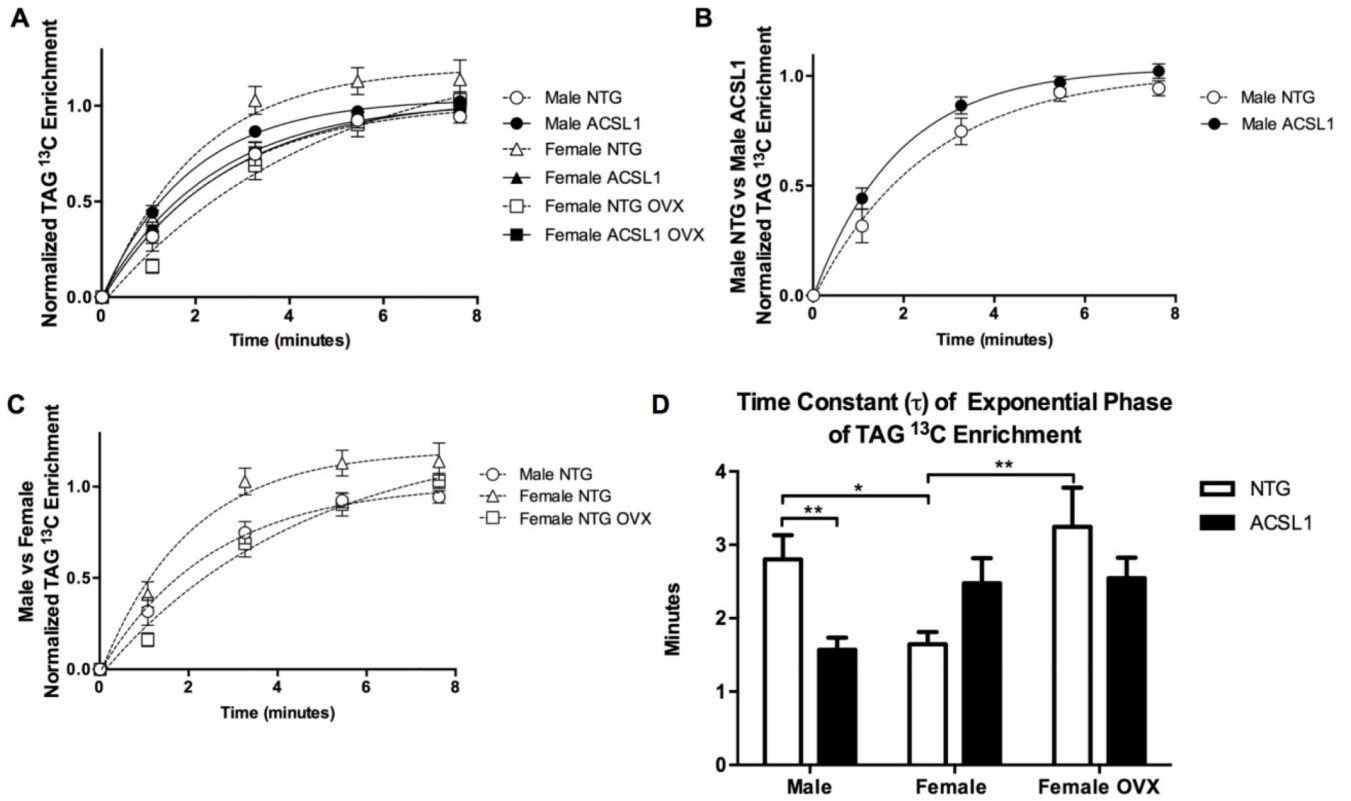


**Figure 2. Kinetics of LCFA uptake are affected by ACSL1 and female sex hormones**  
**(A)** Initial exponential component of <sup>13</sup>C enrichment data normalized to enrichment level.  
**(B)** Initial exponential enrichment phase of TAG in male hearts. Note accelerated <sup>13</sup>C enrichment in male ACSL1 hearts (n = 14) vs male NTG hearts (n = 10). **(C)** Comparison of initial exponential enrichment phases of TAG among male NTG, female NTG, and female NTG OVX. Note accelerated enrichment in Female NTG hearts (n = 9). Sex differences in <sup>13</sup>C enrichment rates are abolished by ovariectomy (female NTG OVX n = 8, female ACSL1 n = 10, female ACSL1 OVX n = 12). **(D)** Time constant,  $\tau$ , of exponential enrichment phase. Values of  $\tau$  lower (faster) in male ACSL1 and female NTG hearts versus male NTG hearts. Ovariectomy increased  $\tau$  values in female NTG and female ACSL1 hearts. Values shown are mean  $\pm$  SEM. \*p<0.05, and \*\*p< 0.01. A waterfall plot of the data is shown in Supplemental Figure 3.

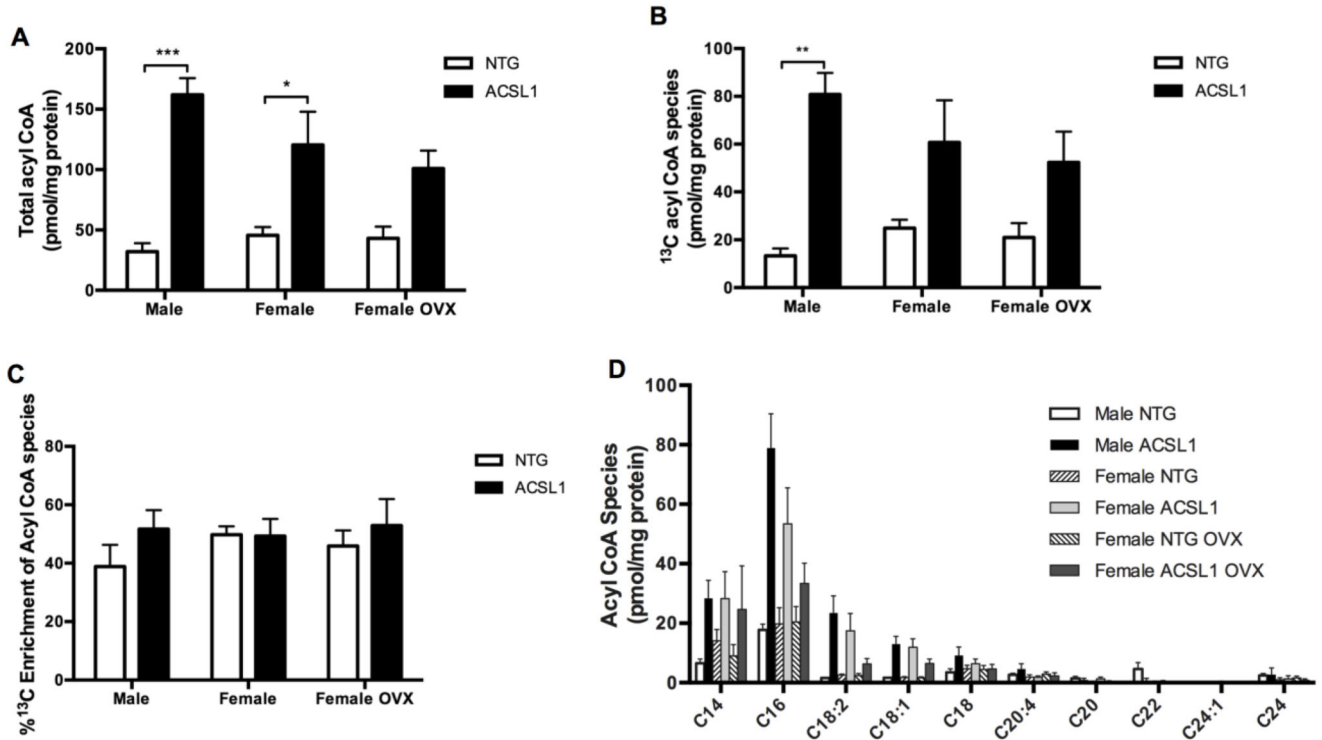


**Figure 3. Cardiac acyl CoA increases with ACSL1 overexpression**

(A) Total acyl CoA content (<sup>12</sup>C and <sup>13</sup>C) of chain lengths 14-24 carbons. Note elevated content in ACSL1 male (n = 6) and ACSL1 female hearts (n = 5) versus male NTG (n = 5) and female NTG hearts (n = 9). (B) Content of <sup>13</sup>C-enriched acyl CoA species. Note greatly elevated content in male ACSL1 hearts. (C) Percent of total acyl CoA pool enriched with <sup>13</sup>C species. Note increased <sup>13</sup>C acyl CoA content despite consistent percent <sup>13</sup>C enrichment of the acyl CoA with ACSL1 overexpression. (D) Distribution of acyl CoA species by chain length. Female NTG OVX n = 6 and female ACSL1 OVX n = 6. \*p < 0.05, \*\*p < 0.01, and \*\*\*p < 0.001.

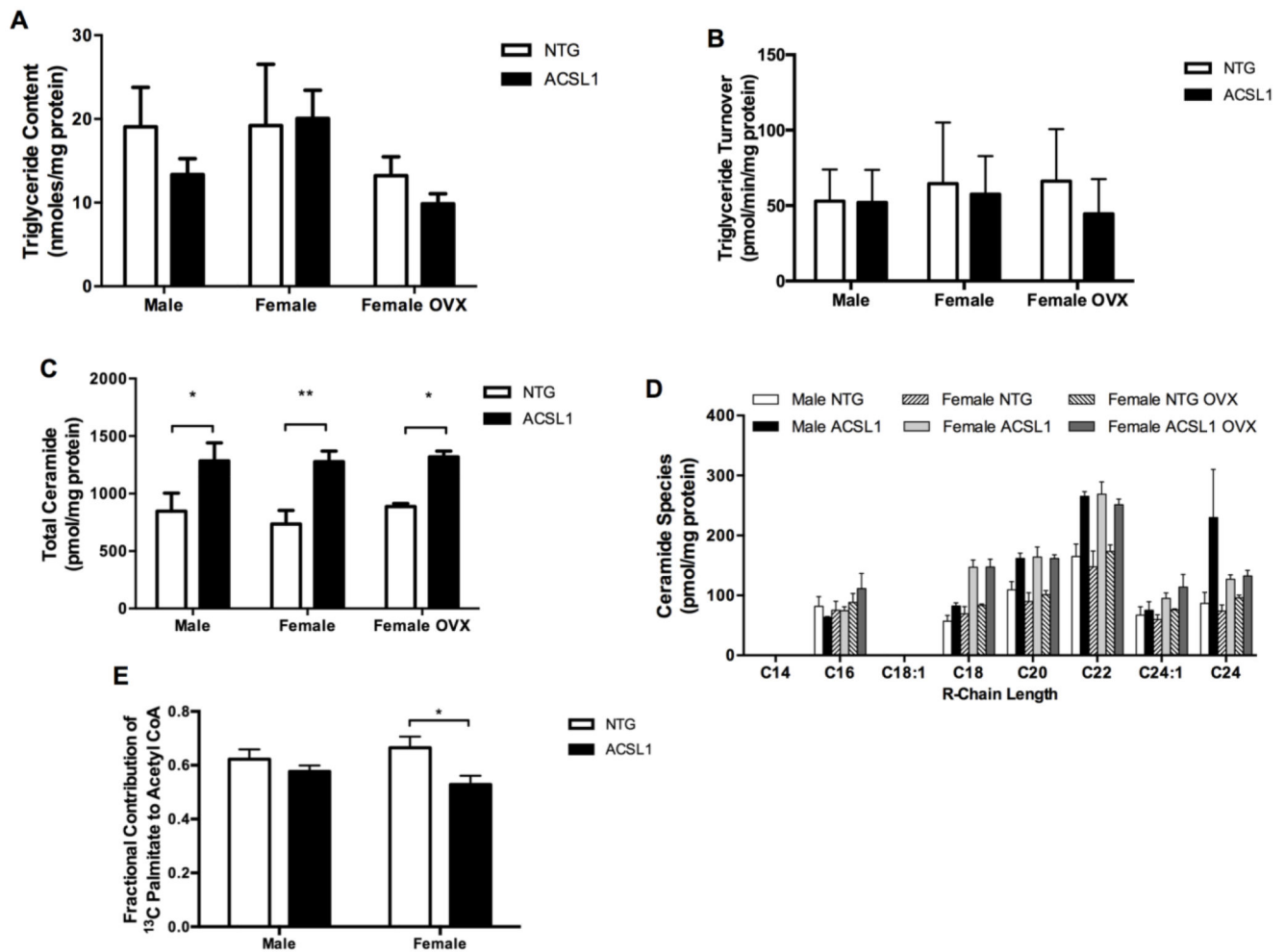


**Figure 4. Acyl derivative formation in the heart is affected by ACSL1 overexpression**  
**(A)** Total cardiac TAG content and **(B)** steady-state turnover of LCFA [ $U\text{-}^{13}\text{C}$ ] palmitate within intramyocardial TAG. Male NTG  $n = 10$ , male ACSL1  $n = 8$ , female NTG  $n = 8$ , female ACSL1  $n = 7$ , female NTG OVX  $n = 6$ , female ACSL1 OVX  $n = 7$ . Accelerated LCFA uptake into cardiomyocytes did not alter TAG formation. ACSL1 and female sex hormone facilitated LCFA uptake, but did not increase LCFA esterification into TAG or TAG lipolysis. **(C)** Total ceramide content was increased by ACSL1 overexpression ( $n = 4$  all). **(D)** Distribution of ceramide species by carbon length of R-chain. Ceramide C22 increased in hearts of all ACSL1 groups, but C24 increased in male ACSL1 hearts only. ACSL1 overexpression specifically increased C22 ceramides irrespective of sex. Formation of C24 ceramide showed sexual dimorphism. **(E)** The fraction of acetyl CoA produced from mitochondrial beta-oxidation of  $^{13}\text{C}$  palmitate was not changed by ACSL1 overexpression in male hearts. Fractional contribution of  $^{13}\text{C}$  palmitate to acetyl CoA decreased in female ACSL1 hearts ( $n = 6$ ) vs female NTG hearts ( $n = 6$ ). Male NTG  $n = 5$  and male ACSL1  $n = 6$ . \* $p < 0.05$ , \*\* $p < 0.01$ .



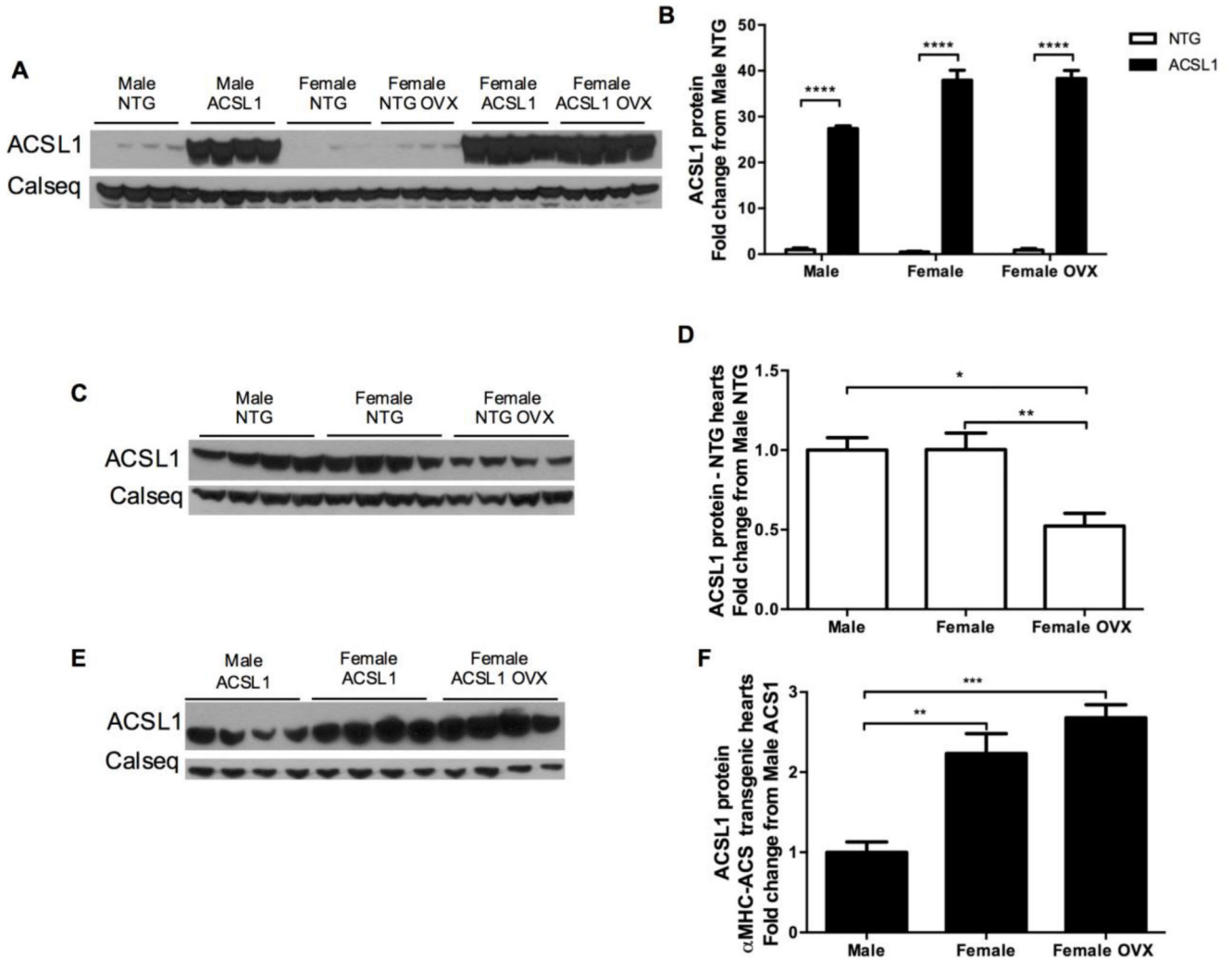


**Figure 5. Cardiac ACSL1 protein expression analysis**

(A and B) Western blot results displaying elevated ACSL1 content ACSL1 hearts versus NTG (n = 4 all). (C and D) Western blot results for ACSL1 content in NTG hearts. ACSL1 protein is similar between NTG males and female hearts, but decreases with ovariectomy (OVX). Female sex hormones are necessary for normal female ACSL1 expression. (E and F) Western blot results showing greater overexpression of ACSL1 in female and female OVX hearts versus male hearts. However, the increase in ACSL1 expression compared to respective NTG hearts was similar among sexes (A and B). Loading normalized to calsequestrin (Calseq) as control. \*p < 0.05, \*\* p < 0.01, \*\*\* p < 0.001, and \*\*\*\* p < 0.0001.

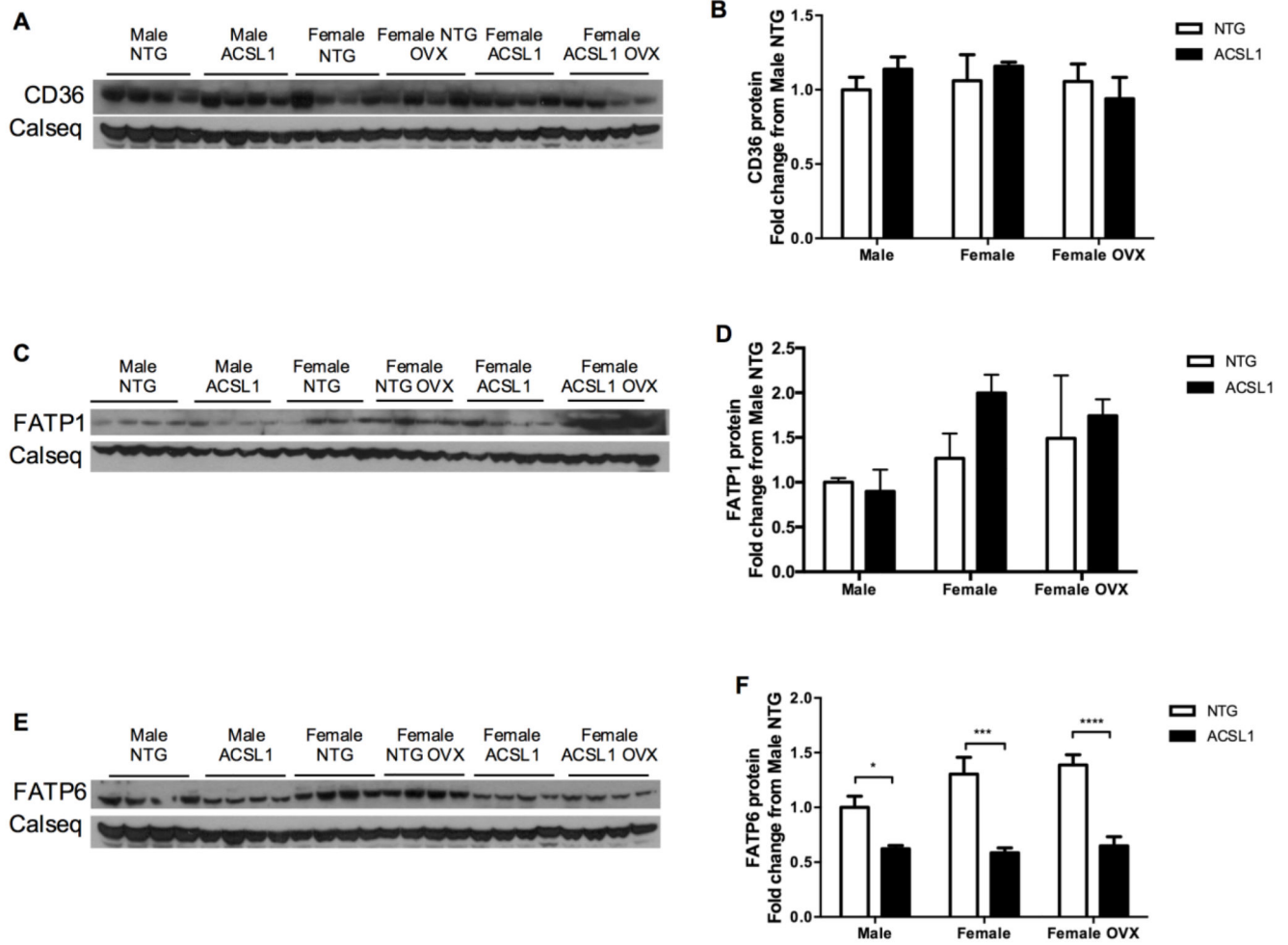


**Figure 6. Protein expression of cardiac sarcolemmal fatty acid transporters**  
 Western immunoblot and quantification for (A, B) CD36, (C, D) FATP1, and (E, F) FATP6 r (n = 4 all). FATP6 content decreased in response to ACSL1 overexpression. Loading normalized to calsequestrin (Calseq) as loading control. \*p < 0.05, \*\*\* p < 0.001, and \*\*\*\* p < 0.0001.